

STRUCTURAL, ELECTRICAL AND OPTICAL STUDIES OF $Zn_xCu_{1-x}S$ ($x = 0.8, 0.6, 0.4$ and 0.2) NANOPARTICLES[†]

✉ **Moly M. Rose^{a,*}, R. Sheela Christy^a, T. Asenath Benitta^a, J. Thampi Thanka Kumaran^b**

^aDepartment of Physics and Research Centre (Reg.No.18123112132030), Nesamony Memorial Christian College, Marthandam, Affiliated to Manonmaniam Sundaranar University, Abishekapatti, Tirunelveli, TamilNadu India, 629165

^bDepartment of Physics and Research Centre, Malankara Catholic College, Mariagiri Kaliyakkavilai, Tamilnadu, India 629163

*Corresponding Author e-mail: molyrengith@gmail.com

Received February 3, 2023; accepted February 16, 2023

$Zn_xCu_{1-x}S$ ($x = 0.8, 0.6, 0.4$ and 0.2) nanoparticles were synthesized by microwave assisted chemical precipitation method. The as-synthesized nanoparticles were characterized by X ray diffraction, SEM and TEM analysis to study the crystal structure, size and surface morphology. The energy dispersed x-ray analysis confirms the presence of Zinc, Copper and Sulphur in proper ratio. The D.C. electrical resistance was measured in the temperature range 300K-500K. All the samples show phase transition above a particular temperature. UV, PL and Raman spectra of all the samples were compared and studied.

Keywords: *chemical precipitation; structural; electrical; phase transition*

PACS: 81.07.-b, 05.70.-a, 81.20.Fw, 61.05.C-, 78.20.-e, 68.37.-d, 81.07.-b, 88.40.H-, 87.64.Ee

1. Introduction

Zinc Sulphide is an important semiconductor material which has been extensively studied because of its physical and chemical properties. ZnS is a wide bandgap semiconductor with a band gap energy of 3.68eV [1,2]. Due to wide band gap, it is useful in optoelectronics [3] and sensors [4]. Zinc Sulphide nanoparticles have potential for various applications in the field of solar cells [5], displays [6], lasers [7] and light emitting diodes, [8] ZnS exist in two phases, i.e's cubic phase and hexagonal phase [9]. Zinc Sulphide nanoparticles have been successfully synthesized by different Methods such as sol-gel [10], sonochemical [11], microwave irradiation [12], microemulsion [13] solvothermal [14] and, hydrothermal [15].

CuS is typical p-type semiconductor that has a direct band gap of 2.5 eV [16-17]. CuS is a potential candidate that could be used in the areas of solar cell elements conversion, gas sensors, IR detectors, electrochemical cells, and photo catalysts [18-22]. The synthesis of copper sulphide has been achieved using different approaches such as microwave irradiation [23], hydrothermal [24], sol-gel [25], microemulsion [26], sonochemical [27], microwave assisted heating [28].

Phase transition in Zinc Sulphide nanoparticles were already studied by varying annealing temperature and pressure, from resistance measurements [29-33]. Phase transition in Copper Sulphide nanoparticles have been studied by previous works [34-35]. $Zn_xCu_{1-x}S$ ($x = 0.8, 0.6, 0.4$ and 0.2) nanoparticles have the application of both Zinc Sulphide nanoparticles and Copper Sulphide nanoparticles. W.Q Peng and G.W Cong investigated the room temperature photoluminescence of (ZnS: Cu) nanoparticles [36]. Jagadeep Kaur and Manoj Sharma studied the structural and optical studies of undoped and copper doped Zinc Sulphide nanoparticles for photocatalytic application [37]. Chanchal Mondal performed ZnS nanoflower promoted evolution of CuS/ZnS p-n heterojunction for exceptional visible light driven photocatalytic activity [38]. S. Harish and J. Archana investigated ultrafast visible light active ZnS/CuS nanostructured photocatalyst [39]. Vijayan et al studied High luminescence efficiency of Copper doped Zinc Sulfide (Cu: ZnS) nanoparticles towards LED applications [40].

In the present study we synthesized $Zn_xCu_{1-x}S$ ($x = 0.8, 0.6, 0.4$ and 0.2) nanoparticles by microwave assisted chemical precipitation method and studied their phase transition through D.C. electrical resistance measurements at various temperatures.

2. Experimental techniques

2.1. Synthesis of $Zn_xCu_{1-x}S$ ($x=0.8, 0.6, 0.4$ and 0.2) nanoparticles by microwave assisted chemical precipitation method

Zinc acetate, Copper acetate and Sodium Sulphide were used for the synthesis of $Zn_xCu_{1-x}S$ ($x = 0.8, 0.6, 0.4$ and 0.2) nanoparticles. Zinc acetate and Copper acetate were taken together in the required composition (1:2 molar ratio) and dissolved in 40 ml distilled water separately and mixed together. The amount of precursor materials taken to dissolve in 80 ml distilled water are given in Table 1. The sodium sulphide solution obtained by dissolving 6.14 gm in 40 ml of distilled water was added in drops to the above solution under effective stirring for 3 hours and kept undisturbed for one day. After performing precipitation, the precipitates were purified out several times, cleaned thoroughly with deionized water several times, and kept in a microwave oven. The solution was then subjected to microwave irradiation of 800 W for 20 minutes. The nanoparticles thus obtained were then brought to room temperature.

[†] Cite as: M.M. Rose, R.S. Christy, T.A. Benitta, and J.T.T. Kumaran, East Eur. J. Phys. 1, 228 (2023), <https://doi.org/10.26565/2312-4334-2023-1-30>
© M.M. Rose, R.S. Christy, T.A. Benitta, J.T.T. Kumaran, 2023

The nanoparticles thus obtained were then cooled to room temperature. Finally, the $Zn_xCu_{1-x}S$ ($x = 0.8, 0.6, 0.4$ and 0.2) nanoparticles were annealed at 100°C for 3 hours to get the phase pure $Zn_xCu_{1-x}S$ ($x = 0.8, 0.6, 0.4$ and 0.2) nanoparticles. The collected nanoparticles were used for different characterization.

Table 1. The amount of precursor materials taken to dissolve in 80 ml distilled water.

Sl no	Expected composition	Zinc acetate	Copper acetate
1	$Zn_{0.8}Cu_{0.2}S$	7.024 gm	1.59 gm
2	$Zn_{0.6}Cu_{0.4}S$	5.26 gm	3.19 gm
3	$Zn_{0.4}Cu_{0.6}S$	3.512 gm	4.79 gm
4	$Zn_{0.2}Cu_{0.8}S$	1.75 gm	6.38 gm

2.2. Instrumentation

X-ray diffraction (XRD) patterns of $Zn_xCu_{1-x}S$ ($x = 0.8, 0.6, 0.4$ and 0.2) nanoparticles were recorded on a powder X-ray diffractometer with Cu $K\alpha$ radiation ($\lambda = 1.54 \text{ \AA}$) with 2θ ranging from angles $10^\circ - 80^\circ$. Surface Morphology of the samples has been studied using TESCAN VEGA3 SBH Scanning Electron Microscope. The elements compositions were confirmed using an energy dispersive X-ray analysis (EDAX) set up attached with scanning electron microscope. A compressed collection of nanoparticles (pellet) was obtained by applying a high pressure of 10 tons/cm^2 . Resistance of the pellet form of the samples were measured using four probe technique. Optical absorption spectra of the synthesized nanoparticles were recorded on UV-visible-spectrometer in the wave length range $200-900 \text{ nm}$. Photoluminescence measurements were performed on Varian Cary Eclipse Photoluminescence spectrophotometer in the range $300-650 \text{ nm}$. Raman spectrum of the $Zn_xCu_{1-x}S$ ($x = 0.8, 0.6, 0.4$ and 0.2) nanoparticles were recorded using peak Seeker Raman spectrometer.

3. Results and discussion

3.1. Structural studies

The indexed XRD patterns of as synthesized $Zn_xCu_{1-x}S$ ($x = 0.8, 0.6, 0.4$ and 0.2) nanoparticles prepared by microwave assisted chemical precipitation method are shown in Fig.1a, 1b, 1c, and 1d respectively. TEM images of all the samples are given in Fig. 2a, 2b, 2c and 2d respectively and it confirms the nanostructures. The respective EDAX images are depicted in Fig. 3a, 3b, 3c and 3d confirms the presence of Zinc, Copper and Sulphur in proper ratio. Samples, structure at room temperature, lattice parameters and particle size of the synthesized samples are given in the Table 2. As the content of Cu increases, the particle size also increases. The XRD patterns of the mixtures show that the mixtures may have the structure of any one of their components (ZnS or CuS).

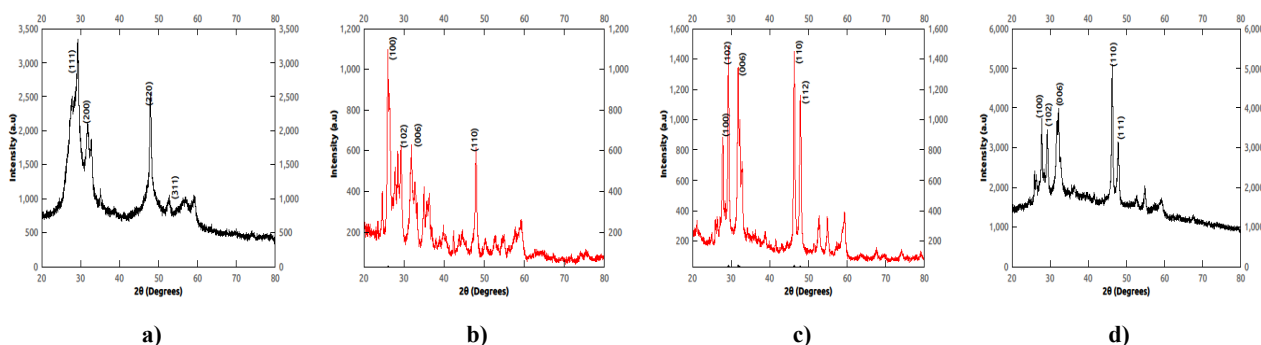
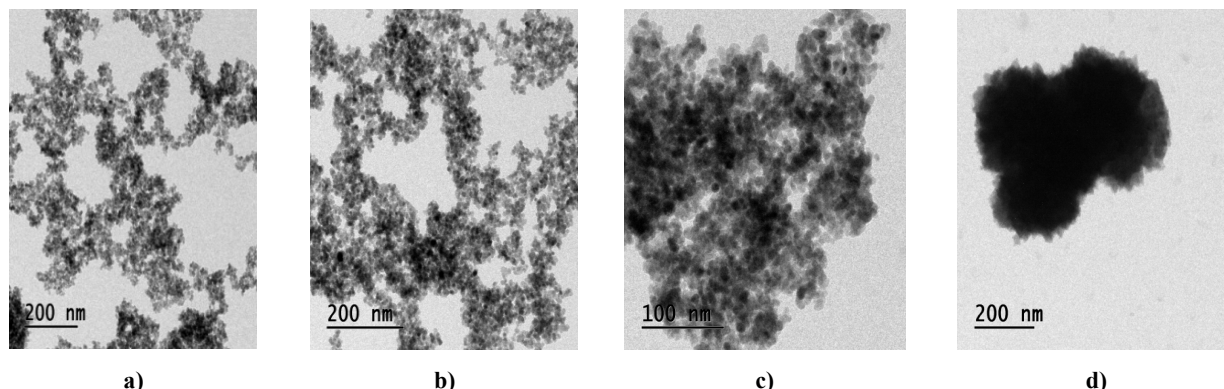


Figure 1. Indexed XRD patterns of nanoparticles

a) $Zn_{0.8}Cu_{0.2}S$ nanoparticles, b) $Zn_{0.6}Cu_{0.4}S$ nanoparticles, c) $Zn_{0.4}Cu_{0.6}S$ nanoparticles, d) $Zn_{0.2}Cu_{0.8}S$ nanoparticles



a)

b)

c)

d)

Figure 2. TEM image of nanoparticles

a) $Zn_{0.8}Cu_{0.2}S$ nanoparticles, b) $Zn_{0.6}Cu_{0.4}S$ nanoparticles, c) $Zn_{0.4}Cu_{0.6}S$ nanoparticles, d) $Zn_{0.2}Cu_{0.8}S$ nanoparticles

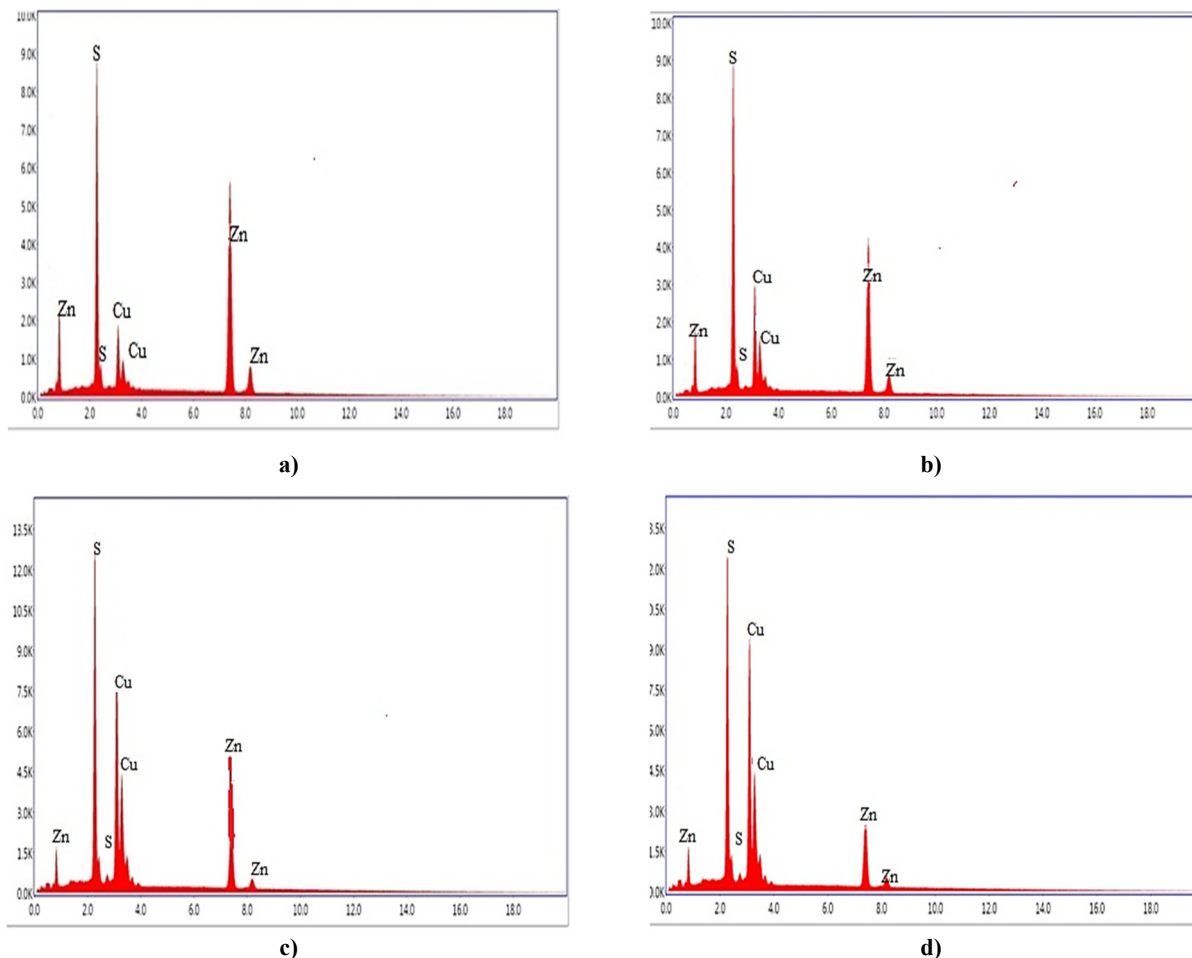


Figure 3. EDAX image of nanoparticles

a) $Zn_{0.8}Cu_{0.2}S$ nanoparticles, b) $Zn_{0.6}Cu_{0.4}S$ nanoparticles, c) $Zn_{0.4}Cu_{0.6}S$ nanoparticles, d) $Zn_{0.2}Cu_{0.8}S$ nanoparticles

Table 2. Samples, structure at room temperature, lattice parameters, particle size of synthesized $Zn_xCu_{1-x}S$ ($x = 0.8, 0.6, 0.4$ and 0.2) nanoparticles

Sl no	Samples	Structure at room temperature	Lattice parameters	Particle size
1	ZnS (reported)	Face centered cubic	$a=b=c=5.4 \text{ \AA}$	
2	$Zn_{0.8}Cu_{0.2}S$	Face centered cubic	$a=b=c=5.2 \text{ \AA}$	31nm
3	$Zn_{0.6}Cu_{0.4}S$	Hexagonal	$a=3.8 \text{ \AA}$ and $c=17 \text{ \AA}$	36nm
4	$Zn_{0.4}Cu_{0.6}S$	Hexagonal	$a=3.9 \text{ \AA}$ and $c=16.8 \text{ \AA}$	39nm
5	$Zn_{0.2}Cu_{0.8}S$	Hexagonal	$a=3.9 \text{ \AA}$ and $c=16.62 \text{ \AA}$	45nm
6	CuS (reported)	Hexagonal	$a=3.8 \text{ \AA}$ and $c=16.4 \text{ \AA}$	

3.2. Electrical Studies

The D.C. electrical resistance of pellet form of the $Zn_xCu_{1-x}S$ ($x=0.8, 0.6, 0.4$ and 0.2) nanoparticles synthesized were measured in the temperature range 300K-500K and is shown in Fig. 4a, 4b, 4c and 4d respectively. A discontinuity is observed in all the samples at a particular temperature due to phase transition [33]. The electrical properties of all the samples also change at this particular temperature. This change in electrical property is due to phase transition [41]. Behaviour of the sample at room temperature, order of resistance at room temperature, possible transition temperatures and behaviour of the sample after phase transition of $Zn_xCu_{1-x}S$ ($x=0.8, 0.6, 0.4, 0.2$) nanoparticles are tabulated in Table 3.

The temperature resistance curve of $Zn_{0.8}Cu_{0.2}S$ nanoparticles (Fig. 4a) remains constant up to 450 K. In this region, the resistance of the sample is of the order of 10^9 Ohms, and the sample behaves as an insulator. Hence it can be utilized for the purpose of withstanding high resistance up to 450 K. As the resistance decreases rapidly with temperature above 450 K it can be used as a temperature sensor.

Fig. 5 shows the order of resistance with variations in the composition of Cu in $Zn_xCu_{1-x}S$ ($x = 0.8, 0.6, 0.4$ and 0.2) nanoparticles. As the composition of Cu in $Zn_xCu_{1-x}S$ ($x = 0.8, 0.6, 0.4$ and 0.2) nanoparticles varies the order of resistance changes from 10^9 to 10^2 Ohms. R. Sheela Christy et al have already reported the rapid decrease in the resistance due to the incorporation of more Cu in CuS-Ag₂S nanoparticle system [42]. From the graph (Fig. 5), as the curve is linear, by varying the composition, the sample can be synthesised with the desired order of resistance for a particular purpose.

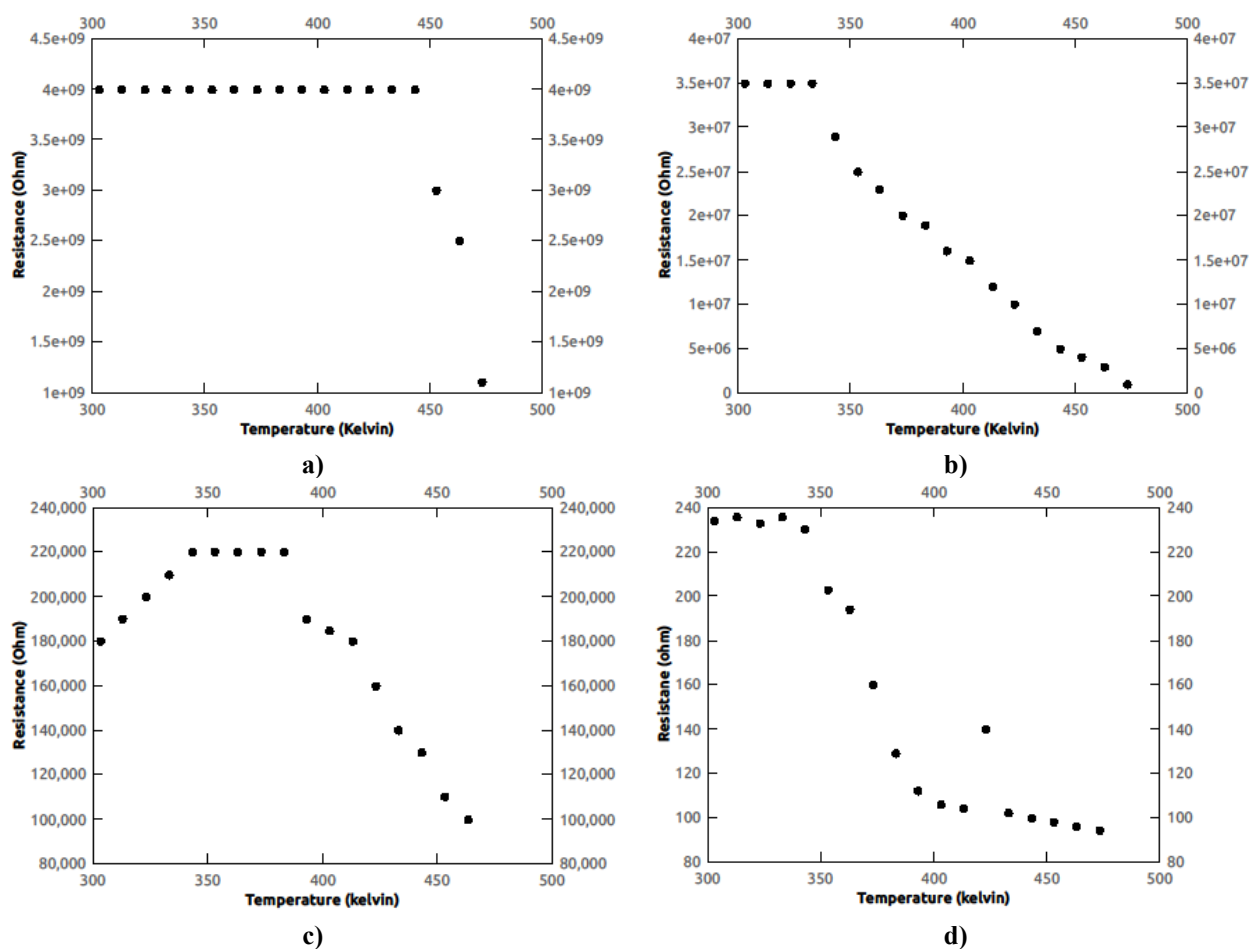


Figure 4. Temperature resistance curve of nanoparticles

a) $Zn_{0.8}Cu_{0.2}S$ nanoparticles, b) $Zn_{0.6}Cu_{0.4}S$ nanoparticles, c) $Zn_{0.4}Cu_{0.6}S$ nanoparticles, d) $Zn_{0.2}Cu_{0.8}S$ nanoparticles

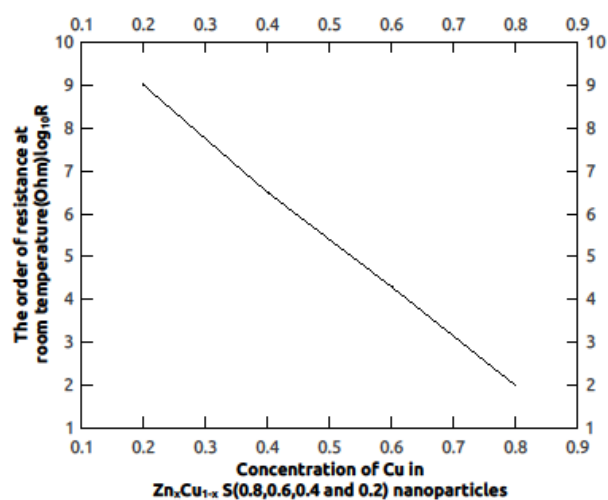


Figure 5. The variation of order of resistance with the composition of Cu in $Zn_xCu_{1-x}S$ ($x=0.8, 0.6, 0.4$ and 0.2) nanoparticles

Table 3. Behaviour of the sample at room temperature, order of resistance at room temperature, possible transition temperatures and behaviour of the sample after phase transition of $Zn_xCu_{1-x}S$ ($x = 0.8, 0.6, 0.4$ and 0.2) nanoparticles

Samples	Behaviour of the sample at room temperature	Order of resistance at room temperature	Possible transition temperatures	Behaviour of the sample after phase transition
$Zn_{0.8}Cu_{0.2}S$	Insulator	$10^9 \Omega$	440K	Semiconductor
$Zn_{0.6}Cu_{0.4}S$	Insulator	$10^7 \Omega$	340K	Semiconductor
$Zn_{0.4}Cu_{0.6}S$	Conductor	$10^5 \Omega$	340K	Semiconductor
$Zn_{0.2}Cu_{0.8}S$	Oscillation	$10^2 \Omega$	340K	Semiconductor

3.3. Optical studies

Fig. 6 shows the optical absorption spectra of $Zn_xCu_{1-x}S$ ($x = 0.8, 0.6, 0.4$ and 0.2) nanoparticles synthesised by microwave-assisted chemical precipitation method. From the absorption spectroscopy, it's clear that when more and more Cu is incorporated, the absorption edge gets shifted towards the lower wavelength region and the percentage of absorption also decreases. The samples can be synthesised with the desired absorption edge and percentage of absorption by varying the composition of Cu in the mixture for different applications.

Fig. 7 depicts the PL emission spectra of $Zn_xCu_{1-x}S$ ($x = 0.8, 0.6, 0.4$ and 0.2) nanoparticles synthesised by microwave-assisted chemical precipitation method. When more Cu is incorporated, the emission peaks shift from 390 nm to 370 nm. Fig. 8 depicts the variation of emission peak with composition of Cu in $Zn_xCu_{1-x}S$ ($x = 0.8, 0.6, 0.4$ and 0.2). Because this variation is linear, $Zn_xCu_{1-x}S$ ($x = 0.8, 0.6, 0.4$ and 0.2) nanoparticles can be tuned to emit different wavelengths in the range 390 nm – 370 nm by varying the composition of Cu, and the sample composition can also be identified from the graph by observing the emission peak.

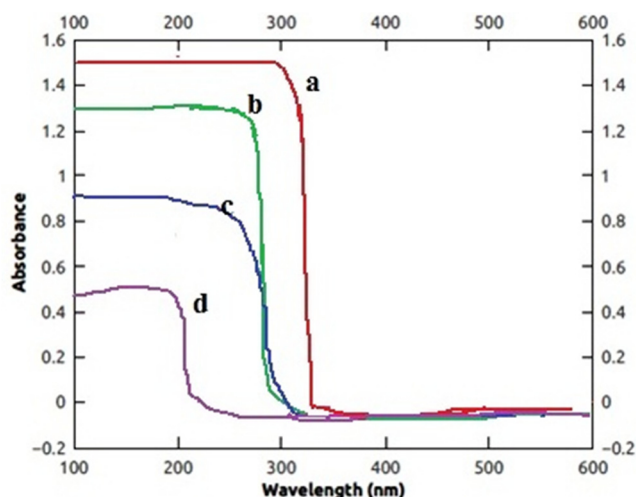


Figure 6. Optical absorption spectrum of nanoparticles
a) $Zn_{0.8}Cu_{0.2}S$ nanoparticles, b) $Zn_{0.6}Cu_{0.4}S$ nanoparticles,
c) $Zn_{0.4}Cu_{0.6}S$ nanoparticles, d) $Zn_{0.2}Cu_{0.8}S$ nanoparticles

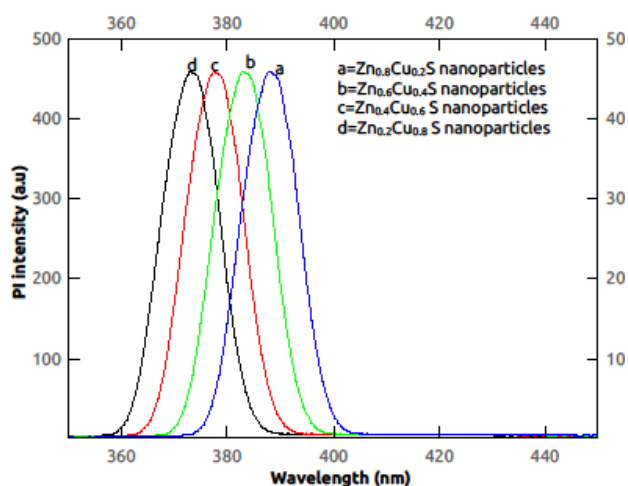


Figure 7. Emission spectra of $Zn_xCu_{1-x}S$ nanoparticles
($x = 0.8, 0.6, 0.4$ and 0.2)

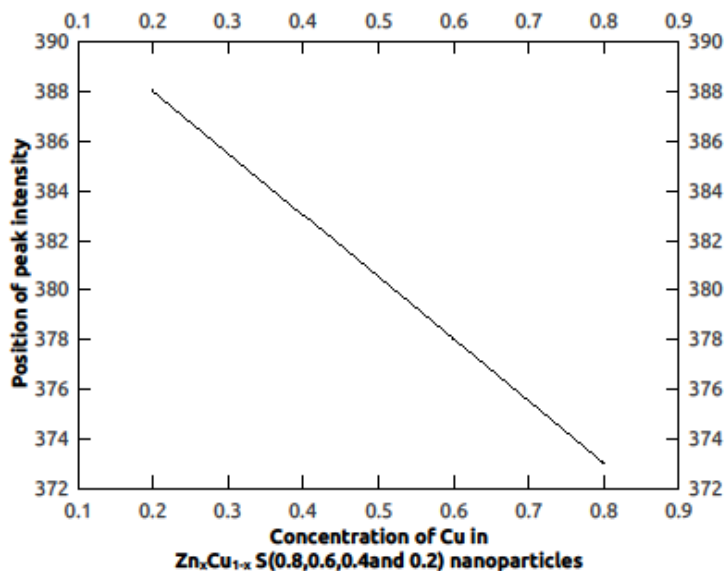


Figure 8. The plot for the variation of emission peak with the composition of Cu in $Zn_xCu_{1-x}S$ ($x = 0.8, 0.6, 0.4$ and 0.2) nanoparticles synthesized by microwave assisted chemical precipitation method

3.4. Raman studies

Figures 9 a-d show the Raman spectra of $Zn_xCu_{1-x}S$ ($x = 0.8, 0.6, 0.4$ and 0.2) nanoparticles synthesised via microwave-assisted chemical precipitation method. The peaks are centered around 340 cm^{-1} and 400 cm^{-1} . When more Cu is incorporated, the intensity of the peaks keeps decreasing. The peak around 290 cm^{-1} was attributed to Cu-S bond vibration [43], and the peak around 400 cm^{-1} was attributed to Zn-S bond vibration [44].

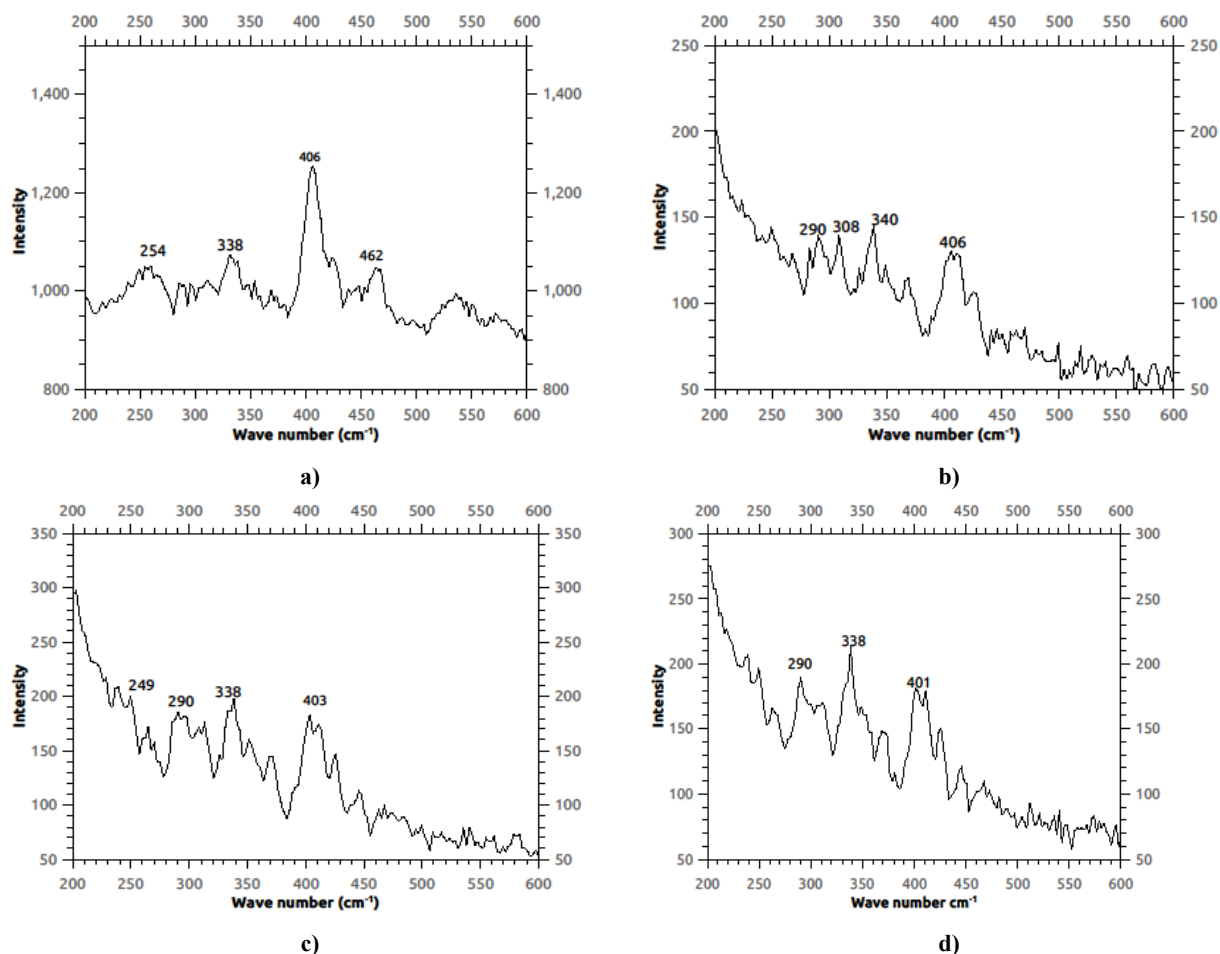


Figure 9. Raman spectrum of nanoparticles

a) $Zn_{0.8}Cu_{0.2}S$ nanoparticles, b) $Zn_{0.6}Cu_{0.4}S$ nanoparticles, c) $Zn_{0.4}Cu_{0.6}S$ nanoparticles, d) of $Zn_{0.2}Cu_{0.8}S$ nanoparticles

4. CONCLUSION

$Zn_xCu_{1-x}S$ ($x = 0.8, 0.6, 0.4$ and 0.2) nanoparticles were synthesised by the microwave-assisted chemical precipitation method. The XRD patterns of the mixtures show that the mixtures may have the structure of any one of their components (ZnS or CuS). The electrical studies show that all the samples undergo phase transition above a particular temperature. Starting with $Zn_{0.8}Cu_{0.2}S$ nanoparticles, the electrical resistance of the samples is rapidly reduced as more and more Cu is incorporated. From the absorption spectroscopy, it's clear that as more and more Cu is incorporated, the absorption edge gets blue-shifted. By varying the composition of Cu , the mixture can be tuned to emit different wavelengths in the range of 390 nm to 370 nm. The peaks of both ZnS and CuS are present in the Raman spectra of the $Zn_xCu_{1-x}S$ ($x = 0.8, 0.6, 0.4$ and 0.2) nanoparticles.

Acknowledgements

The authors gratefully acknowledge Nesamony Memorial Christian College, Marthandam, for providing the necessary laboratory facilities to carry out this work.

Funding. This study was done towards the Ph.D. work of Mrs. Moly M Rose and was not funded by any external agencies.

Competing Interests. We have not received any funding from any company or university, and hence, there is no conflict of interest.

Author Contributions. All authors discussed the results and contributed to the final manuscript.

Data availability statement. The data that support the findings of this study are available within the article

ORCID IDs

©Moly M. Rose, <https://orcid.org/0000-0003-4840-0567>

REFERENCES

- [1] X.D. Gao, X.M. Li, and W.D. Yu, "Morphology and optical properties of amorphous ZnS films deposited by ultrasonic-assisted successive ionic layer adsorption and reaction method", *Thin Solid Films*, **468**, 43 (2004). <https://doi.org/10.1016/j.tsf.2004.04.005>
- [2] I. Parvaneh, S. Samira, and N. Mohsen, "Characterization of ZnS nanoparticles synthesized by co-precipitation method", *Chinese Physics B*, **24**(4), 046104 (2015). <https://doi.org/10.1088/1674-1056/24/4/046104>

- [3] U.P. Onochie, S.C. Ikpeseni, A.E. Igweoko, H.I. Owamah, C.C. Aluma, and C. Augustine, "Optical Properties of Zinc Sulphide Thin Films Coated with Aqueous Organic Dye Extract for Solar and Optoelectronic Device Applications", *Journal of Electronic Materials*, **50**, 2576 (2021). <https://doi.org/10.1007/s11664-021-08792-0>
- [4] S.K. Mehta, Khushboo, and A. Umar, "Highly sensitive hydrazine chemical sensor based on mono-dispersed rapidly synthesized PEG-coated ZnS nanoparticles", *Talanta*, **85**(5), 2411 (2011). <https://doi.org/10.1016/j.talanta.2011.07.089>
- [5] M. Ragam, N. Sankar, and K. Ramachandran, "Investigation on Zinc Sulphide Nanoparticles in Dye Sensitized Solar Cell", *AIP Conference Proceedings*, **1349**, 411 (2011). <https://doi.org/10.1063/1.3605909>
- [6] H. Ali, S. Karim, M.A. Rafiq, K. Maaz, A.U. Rahman, A. Nisar, and M. Ahmad, "Electrical conduction mechanism in ZnS nanoparticles", *J. Alloys Compd.* **612**, 64 (2014). <https://doi.org/10.1016/j.jallcom.2014.05.163>
- [7] M. Jayalakshmi, and M.M. Rao, "Synthesis of zinc sulphide nanoparticles by thiourea hydrolysis and their characterization for electrochemical capacitor applications", *Journal of Power Sources*, **157**(1), 624 (2006). <https://doi.org/10.1016/j.jpowsour.2005.08.001>
- [8] S. Vijayan, G. Umadevi, R. Mariappan, M. Narayanan, B. Narayanamoorthy, and S. Kandasamy, "High luminescence efficiency of Copper doped Zinc Sulfide (Cu: ZnS) nanoparticles towards LED applications", *Materials Today: Proceedings*, (2020). <https://doi.org/10.1016/j.matpr.2020.11.214>
- [9] T.T.Q. Hoa, L.V. Vu, T.D. Canh, and N.N. Long, "Preparation of ZnS nanoparticles by hydrothermal method", *Journal of Physics: Conference Series*, **187**, 012081 (2009). <https://doi.org/10.1088/1742-6596/187/1/012081>
- [10] L. Kashinath, K. Namratha, S. Srikantaswamy, A. Vinu, and K. Byrappa, "Microwave treated sol-gel synthesis and characterization of hybrid ZnS-RGO composites for efficient photodegradation of dyes", *New J. Chem.* **41**, 1723 (2017). <https://doi.org/10.1039/C6NJ03716J>
- [11] J.-R. Li, J.-F. Huang, L.-Y. Cao, J.-P. Wu, and H.-Y. He, "Synthesis and kinetics research of ZnS nanoparticles prepared by sonochemical process", *Material science and Technology*, **26**, 1269 (2013). <https://doi.org/10.1179/026708309X12495548508428>
- [12] S. Thangavel, K. Krishnamoorthy, S.-J. Kim, and G. Venugopal, "Designing ZnS decorated reduced graphene-oxide nanohybrid via microwave route and their application in photocatalysis", *Journal of Alloys and Compounds*, **683**, 456 (2016). <https://doi.org/10.1016/j.jallcom.2016.05.089>
- [13] T. Charinpanitkul, A. Chanagul, J. Dutta, U. Rungsardthong, and W. Tanthapanichakoon, "Effects of cosurfactant on ZnS nanoparticle synthesis in microemulsion", *Science and Technology of Advanced Materials*, **6**, 266 (2005). <https://doi.org/10.1016/j.stam.2005.02.005>
- [14] F.A. La Porta, M.M. Ferrer, Y.V.B. Santana, C.W. Raubach, V.M. Longo, J.R. Sambrano, E. Longo, et al., "Synthesis of wurtzite ZnS nanoparticles using the microwave assisted solvothermal method", *Journal of Alloys and Compounds*, **556**, 153 (2013). <http://dx.doi.org/10.1016/j.jallcom.2012.12.081>
- [15] T.T.Q. Hoa, L.V. Vu, T.D. Canh, and N.N. Long, "Preparation of ZnS nanoparticles by hydrothermal method", *IOP Publishing Journal of Physics, Conference Series*, **187**, 012081 (2009). <https://doi.org/10.1088/1742-6596/187/1/012081>
- [16] I. Puspitasari, T.P. Gujar, K.-D. Jung, and, O.-S. Joo, "Simple chemical preparation of CuS nanowhiskers", *Materials Science and Engineering B*, **140**, 199 (2007). <https://doi.org/10.1016/j.mseb.2007.04.012>
- [17] F. Ghribi, A. Alyamani, Z.B. Ayadi, K. Djessas, L. ELMir, "Study of CuS Thin Films for Solar Cell Applications Sputtered from Nanoparticles Synthesised by Hydrothermal Route", *Energy Procedia*, **84**, 197203 (2015). <https://doi.org/10.1016/j.egypro.2015.12.314>
- [18] H. Wang, Y. Sun, W. Yue, Q. Kang, H. Li, and D. Shen, "A smartphone-based double-channel fluorescence setup for immunoassay of a carcinoembryonic antigen using CuS nanoparticles for signal amplification", *Analyst*, **143**, 1670 (2018). <https://doi.org/10.1039/C7AN01988B>
- [19] M.P. Ravele, O.A. Oyewo, and D.C. Onwudiwe, "Controlled Synthesis of CuS and Cu₉S₅ and Their Application in the Photocatalytic Mineralization of Tetracycline", *Catalysts*, **11**, 899 (2021). <https://doi.org/10.3390/catal11080899>
- [20] D. Ayodhya, and G. Veerabhadram, "Investigation of temperature and frequency dependence of electrical conductivity and dielectric behavior in CuS and rGO capped CuS nanocomposites", *Mater. Res. Express*, **6**, 045910 (2019). <https://doi.org/10.1088/2053-1591/aaf555>
- [21] Z. Zha, S. Zhang, Z. Deng, Y. Li, C. Lia, and Z. Dai, "Enzyme-Responsive Copper Sulphide Nanoparticles for Combined Photoacoustic Imaging", *Chem. Commun.* **49**, 3455 (2013). <https://doi.org/10.1039/C3CC40608C>
- [22] S. Goel, F. Chen, and W. Cai, "Synthesis and Biomedical Applications of Copper Sulfide Nanoparticles: From Sensors to Theranostics", *Nano Micro Small*, **10**(4), 631 (2014). <https://doi.org/10.1002/sml.201301174>
- [23] M. Nafees, S. Ali, S. Idrees, K. Rashid, M.A. Shafique, "A simple microwave assisted aqueous route to synthesis CuS nanoparticles and further aggregation to spherical shape", *Applied Nanoscience*, **3**, 119 (2013). <https://doi.org/10.1007/s13204-012-0113-9>
- [24] M. Saranya, C. Santhosh, R. Ramachandran, and A.N. Grace, "Growth of CuS Nanostructures by Hydrothermal Route and Its Optical Properties", *Journal of Nanotechnology*, **2014**, 321571 (2014). <https://doi.org/10.1155/2014/321571>
- [25] S. Riyaz, A. Parveen, and A. Azam, "Microstructural and optical properties of CuS nanoparticles prepared by sol-gel route", *Perspectives in Science*, **8**, 632 (2016). <https://doi.org/10.1016/j.pisc.2016.06.041>
- [26] J.N. Solanki, R. Sengupta, Z.V.P. Murthy, "Synthesis of copper sulphide and copper nanoparticles with microemulsion method", *Solid State Sciences*, **12**(9), 1560 (2010). <https://doi.org/10.1016/j.solidstatesciences.2010.06.021>
- [27] A.S.R. Manivannan, and S.N. Victoria, "Simple one-pot sonochemical synthesis of copper sulphide nanoparticles for solar cell applications", *Arabian Journal of Chemistry*, **12**(8), 2439 (2019). <https://doi.org/10.1016/j.arabjc.2015.03.013>
- [28] X.-H. Liao, N.-Y. Chen, S. Xu, S.-B. Yang, J.-J. Zhu, "A microwave assisted heating method for the preparation of copper sulfide nanorod", *Journal of Crystal Growth*, **252**(4), 593 (2003). [https://doi.org/10.1016/S0022-0248\(03\)01030-3](https://doi.org/10.1016/S0022-0248(03)01030-3)
- [29] A.K. Kole, and P. Kumbhakar, "Cubic-to-hexagonal phase transition and optical properties of chemically synthesized ZnS nanocrystals", *Results in Physics*, **2**, 150 (2012). <http://dx.doi.org/10.1016/j.rinp.2012.09>
- [30] J. Kennedy, P.P. Murmu, P.S. Gupta, D.A. Carder, S.V. Chong, J. Leveneur, and S. Rubanov, "Effects of annealing on the structural and optical properties of zinc sulfide thin films deposited by ion beam sputtering", *Materials Science in Semiconductor Processing* **26**, 561 (2014). <http://dx.doi.org/10.1016/j.mssp.2014.05.055>

- [31] Y. Li, W. Tan, and Y. Wu, "Phase Transition between Sphalerite and Wurtzite in ZnS", *Optical Ceramic Materials*, 40(5), 2130 (2020). <https://doi.org/10.1016/j.jeurceramsoc.2019.12.045>
- [32] C. Yang, Y. Liu, H. Sun, D. Guo, X. Li, W. Li, B. Liu, and X. Zhang, "Pressure-induced transition-temperature reduction in ZnS nanoparticles", *Nanotechnology*, 19, 095704 (2008). <https://doi.org/10.1088/0957-4484/19/9/095704>
- [33] M.M. Rose, R.S. Christy, T.A. Benitta, J.T.T. Kumaran, and M.R. Bindhu, "Phase transition in ZnS nanoparticles: electrical, thermal, structural, optical, morphological, antibacterial and photocatalytic properties", *Chalcogenide Letters*, 19(11), 855 (2022). <https://doi.org/10.15251/CL.2022.1911.855>
- [34] P.V. Quintana-Ramirez, Ma.C. Arenas-Arrocena, J.Santos-Cruz, M. Vega-González, O. Martínez-Alvarez, V.M. Castaño-Meneses, L.S. Acosta-Torres, and J. de la Fuente-Hernández, "Growth evolution and phase transition from chalcocite to digenite in nanocrystalline copper sulfide: Morphological, optical and electrical properties", *Beilstein J. Nanotechnol.* 5, 1542 (2014). <https://doi.org/10.3762/bjnano.5.166>
- [35] A. Narjis, A. Outzourhit, A. Aberkouks, M. El Hasnaoui, and L. Nkhaili, "Structural and thermoelectric properties of copper sulphide powders", *Journal of Semiconductors*, 39(12), (2018). <https://doi.org/10.1088/1674-4926/39/12/122001>
- [36] W.Q. Peng, G.W. Cong, S.C. Qu, and Z.G. Wang, "Synthesis and photoluminescence of ZnS:Cu nanoparticles", *Optical Materials* 29, 313 (2006). <https://doi.org/10.1016/j.optmat.2005.10.003>
- [37] J. Kaur, M. Sharma, and O.P. Pandey, "Structural and optical studies of undoped and copper doped zinc sulphide nanoparticles for photocatalytic application", *Superlattices and Microstructures*, 77, 35 (2015). <https://dx.doi.org/10.1016/j.spmi.2014.10.032>
- [38] C. Mondal, A. Singh, R. Sahoo, A.K. Sasmal, Y. Negishib, and T. Pal, "Preformed ZnS nanoflower prompted evolution of CuS/ZnS p-n heterojunctions for exceptional visible-light driven photocatalytic activity", *Royal society for chemistry, New J. Chem.* 39, 5628 (2015). <https://doi.org/10.1039/c5nj00128e>
- [39] S. Harish, J. Archana, M. Navaneethan, S.P.A. Singh, V. Gupta, D.K. Aswal, H. Ikeda, and Y. Hayakawa, "Synergetic effect of CuS@ZnS nanostructures on photocatalytic degradation of organic pollutant under visible light irradiation", *RSC Adv.* 7, 34366 (2017). <https://doi.org/10.1039/c7ra04250g>
- [40] S. Vijayan, G. Umadevi, R. Mariappan, M. Narayanan, B. Narayanamoorthy, and S. Kandasamy, "High luminescence efficiency of Copper doped Zinc Sulfide (Cu: ZnS) nanoparticles towards LED applications", *Materials Today: Proceedings*, (2020). <https://doi.org/10.1016/j.matpr.2020.11.214>
- [41] R.S. Christy, and J.T. Thankakumaran, "Phase transition in CuS nanoparticles", *Journal of Non-Oxide Glasses*, 6(1), 13 (2016). https://chalcogen.ro/13_Sheela.pdf
- [42] R.S. Christy, J.T. Thankakumaran, and C. Bansal, "Jump in Band Gap Energy of Ag₂S Nanoparticles Synthesised by Solvothermal Method", *Advanced science focus*, 2(2), 115 (2014). <https://doi.org/10.1166/asfo.2014.1087>
- [43] T. Hurma, and S. Kose, "XRD Raman analysis and optical properties of CuS nanostructured film", *Optik - International Journal for Light and Electron Optics*, 127(15), 6000 (2006). <https://doi.org/10.1016/j.ijleo.2016.04.019>
- [44] S.S. Kumar, M.A. Khadar, S.K. Dhara, T.R. Ravindran, and K.G.M. Nair, "Photoluminescence and Raman studies of ZnS nanoparticles implanted with Cu⁺ ions", *Nuclear Instruments and Methods in Physics Research B*, 251, 435 (2006). <https://doi.org/10.1016/j.nimb.2006.07.002>

СТРУКТУРНІ, ЕЛЕКТРИЧНІ ТА ОПТИЧНІ ДОСЛІДЖЕННЯ НАНОЧАСТИНОК $Zn_xCu_{1-x}S$ ($x = 0,8, 0,6, 0,4$ та $0,2$)

Моли М. Роуз^а, Р. Шила Крісті^а, Т. Асенат Бенітта^а, Дж. Тампі Танка Кумаран^б

^аДепартамент фізики та науково-дослідний центр (реєстр. № 18123112132030), Меморіальний християнський коледж Несамоні, Мартадам, філія університету Манонманіам Сундаранар

Абішекапатті, Тірунелвелі, Таміл Наду, Індія, 629165

^бДепартамент фізики та науково-дослідний центр, Католицький коледж Маланкара,

Маріагірі Каліяккавілай, Тамілнаду, Індія 629163

Наночастинки $Zn_xCu_{1-x}S$ ($x = 0,8, 0,6, 0,4$ і $0,2$) були синтезовані методом хімічного осадження за допомогою мікрохвиль. Синтезовані наночастинки були охарактеризовані за допомогою дифракції рентгенівських променів, SEM та TEM аналізу для вивчення кристалічної структури, розміру та морфології поверхні. Енергодисперсний рентгенівський аналіз підтверджує наявність цинку, міді та сірки в правильному співвідношенні. Електричний опір постійному струму вимірювали в діапазоні температур 300-500 К. Усі зразки демонструють фазовий перехід вище певної температури. УФ, ФЛ та спектри комбінаційного розсіювання всіх зразків були порівняні та досліджені.

Ключові слова: хімічне осадження; структурний; електричні; фазовий перехід